Ultrafast spectroscopic studies in polyfluorene: [6,6]-phenyl C_{61}-butyric acid methyl ester blend films: monitoring the photoinduced charge transfer process

2004 J. Phys.: Condens. Matter 16 8105

(http://iopscience.iop.org/0953-8984/16/45/033)

INSTITUTE OF PHYSICS PUBLISHING JOURNAL OF PHYSICS: CONDENSED MATTER

J. Phys.: Condens. Matter **16** (2004) 8105–8116 PII: S0953-8984(04)75782-3

Ultrafast spectroscopic studies in polyfluorene: [6,6]-phenyl C_{61}-butyric acid methyl ester blend films: monitoring the photoinduced charge transfer process

Roberto Pacios[1], Jenny Nelson[1], Donal D C Bradley[1,4], Tersilla Virgili[2], Guglielmo Lanzani[2] and Christoph J Brabec[3]

[1] Centre for Electronic Materials and Devices, Imperial College London, The Blackett Laboratory, Prince Consort Road, London SW7 2BZ, UK
[2] Dipartimento di Fisica, Politecnico di Milano, Piazza L da Vinci 32, I-20133 Milano, Italy
[3] SIEMENS AG, CT MM1, Innovative Polymers, Paul Gossenstrasse 100, D-91052 Erlangen, Germany

E-mail: d.bradley@imperial.ac.uk

Received 30 January 2004, in final form 26 August 2004
Published 29 October 2004
Online at stacks.iop.org/JPhysCM/16/8105
doi:10.1088/0953-8984/16/45/033

Abstract

We present a study of charge transfer in polyfluorene: [6,6]-phenyl C_{61}-butyric acid methyl ester (PCBM) blend films. After photoexciting the conjugated polymer, electrons are very quickly transferred onto the PCBM leaving positive charges in the polymer. The presence of new photogenerated species in both polymer and PCBM can be demonstrated by photoinduced optical absorption studies. Using ultrafast spectroscopic experiments, not only are we able to demonstrate the charge transfer process in such composites but also we can time resolve the dynamics of the process. Charge transfer is, in this way, estimated to take place ∼4 ps after photoexcitation. After ∼120 ps all charges have already been transferred and the process concludes. The resulting separated charges have the potential to produce a photocurrent if they are successfully driven through the bulk and collected by suitable electrodes.

1. Introduction

Blends of conjugated polymers with PCBM have been demonstrated as one of the most promising systems for solar energy conversion into electricity. An external quantum efficiency of 76% [1], and power conversion efficiencies of over 3.0% [2, 3] under AM1.5 illumination conditions have been reported. Polyfluorenes are emerging as one of the most promising classes of conjugated polymers due to good transport characteristics [4], and thermal stability.

[4] Author to whom any correspondence should be addressed.

Dioctylfluorene units are often copolymerized with other conjugated units in order to modify their electronic and optical properties. Addition of arylamine units considerably improves the hole transport properties of the material and lowers the ionization potential [4]. When a benzothiadiazole unit is added instead, the transport properties of the materials are modified to also enable electron transport. F8BT is an electron transport material with an impressive electron mobility [5]. The Dow Chemical Company proprietary Red F copolymer similarly combines both electron and hole transport functionality and the electron and hole mobility are then of the same order of magnitude [6]. In Red F, a minority red chromophore unit is also included, producing a somewhat complex red emitting polyfluorene based copolymer. Photovoltaic devices made from similar red polyfluorenes have led to efficient photocurrent generation and power conversion efficiencies of up to 2% [7, 8]. When used as the electron donating component in polymer/fullerene blend devices, these red polyfluorenes offer relatively high open-circuit voltages, on account of their relatively high ionization potentials, and as such offer potential advantages over other red polymers.

In this paper we report ultrafast spectroscopic studies on Red F and Red F:PCBM (10 mol% PCBM in Red F) films. Films were spin coated on glass substrates from chloroform solutions giving thicknesses of ∼200–300 nm. The femtosecond laser system consists of a mode-locked Ti:sapphire laser with chirped pulse amplification, providing 150 fs pulses at 780 nm (1.6 eV) at a repetition rate of 1 kHz. The pump pulses at 390 nm (3.2 eV) with intensity of 250 μJ cm^{-2} were obtained by frequency doubling the beam in a 1 mm thick LiB_3O_5 crystal. The white light probe beam was generated by focusing a small fraction of the fundamental beam into a 1 mm thick sapphire plate. For a fixed pump and probe delay, the whole white light pulse was spectrally analysed (after passing through the sample) using a monochromator and a silicon diode array. Differential transmission spectra were obtained by subtracting pump-on and pump-off data. Temporal evolution of the differential transmission was recorded at selected wavelengths (using interference filters of 10 nm bandwidth) by a standard lock-in technique [9].

2. Results and discussion

2.1. Pristine Dow Red F

Figure 1 shows the ground state absorption and photoluminescence (PL) spectra of films of pure Red F. The absorption spectrum has two peaks at 290 nm (1.91 eV) and 437 nm (2.85 eV) which are also observed in F8BT [10]. Additionally, there is a shoulder due to the absorption of the red chromophore that reaches out to 600 nm (2.07 eV). The PL peaks in the red part of the spectrum at 645 nm (1.92 eV), with a vibronic shoulder at 690 nm (1.79 eV). Figure 2 shows the $\Delta T/T$ spectra of pure Red F for different time delays between the pump and probe beam. Three main features can be observed:

(i) A positive peak at 560 nm (2.21 eV); this peak is located in the spectral region in which there is polymer ground state absorption, and is therefore assigned mainly to photobleaching of the ground state species, although, as we shall discuss below, there also appears to be a contribution from polaron absorbance. This feature will be hereafter referred to as PB.

(ii) A negative peak at 650 nm (1.91 eV), labelled PA1. When Red F was oxidized with $SbCl_5$ (see figure 3), an absorption band of the Red F$^+$ was found to be in this same part of the spectrum. Hence, PA1 is assigned to positive polaron states.

(iii) A negative peak at 850 nm (1.46 eV), labelled PA2. The assignment of this feature requires a comparison of the dynamics of the features observed in the spectrum (figure 4).

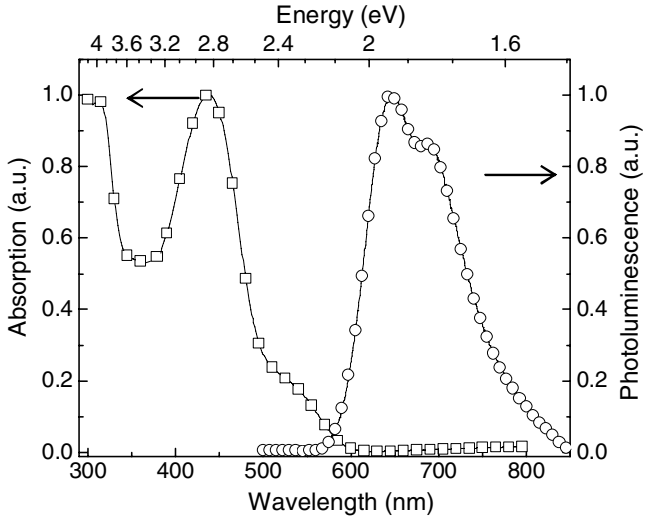

Figure 1. Room temperature ground state optical absorption (squares) and photoluminescence emission (circles) spectra for Dow Red F thin films.

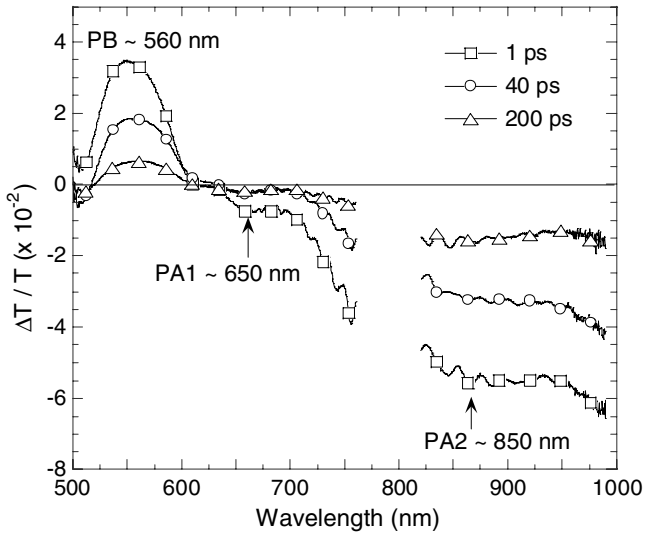

Figure 2. $\Delta T/T$ spectra of pure Dow Red F for different time delays between the pump and probe beams. The data were taken at room temperature, with a pump beam intensity, $I_{\mathrm{PUMP}} \sim 250\ \mu\mathrm{J\ cm^{-2}}$. The excitation wavelength was $\lambda_{\mathrm{exc}} = 390$ nm and the pump duration was 150 fs.

It can be seen that the decay of PB and PA2 is very similar. Following previous work in which the dynamics of $S_1 \rightarrow S_n$ transitions (singlet excited state absorption) were compared to $S_1 \rightarrow S_0$ transitions (stimulated emission) [11–13], and given the close similarity here of the PB and PA2 decays (figure 4), we assign PA2 mainly to singlet excited state absorption. Because the absorption spectrum of the positive polaron in Red F is broad (figure 3) we expect a contribution to both PB and PA2 from positive polaron absorption in addition to the contributions from ground state bleaching and singlet absorption, respectively.

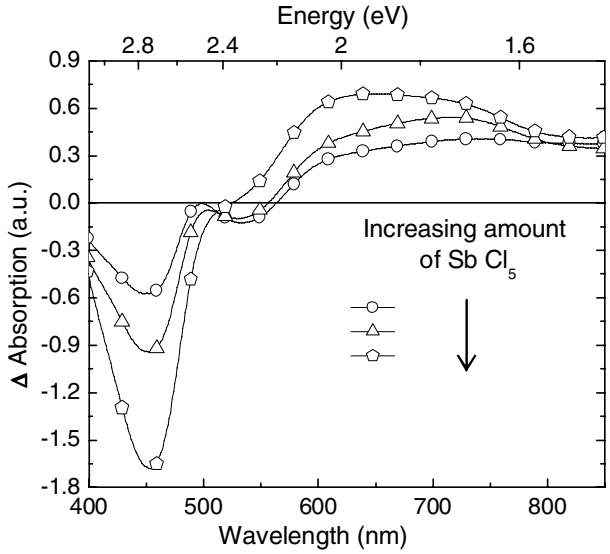

Figure 3. Absorption spectra of $SbCl_5$ doped Dow Red F in chloroform solution. The absorption spectrum of the pure polymer was used as a reference and subtracted from the spectra for the different $SbCl_5$ solutions to determine Δ absorption spectra for comparison with the $\Delta T/T$ data.

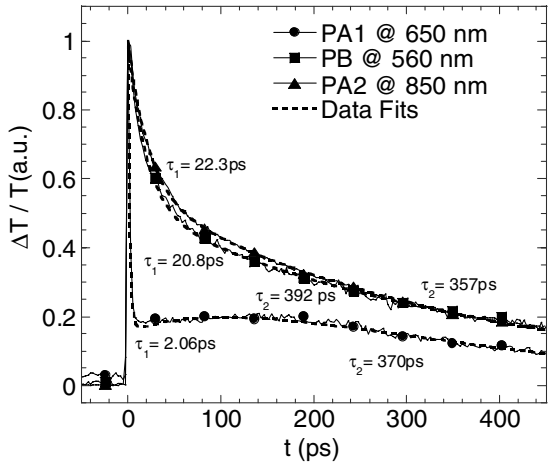

Figure 4. Dynamics of the features observed in the $\Delta T/T$ spectra for pure Dow Red F. The lifetimes obtained by fitting the experimental results to different exponential decays are also shown as are the fits (dashed curves). The dynamics were normalized by using the experimentally measured data at $t = 0$; PA2 = 81.3, PB = 52.06, PA1 = 53.7.

Figure 4 shows the dynamics of the three main features measured on a timescale between 0 (excitation time) and 400 ps after photoexcitation by the pump beam. Experimental results were also fitted to exponential decays in order to calculate the lifetimes of the species involved. As already remarked, PB and PA2 are considered to arise primarily from the same species. Their decays can be fitted to double exponentials with very similar lifetimes for both features. The initial amplitude of PA1 shows that polaron pairs have been generated on a timescale faster than 1 ps by the laser pulse. Such prompt charge pair generation can result from the

dissociation of higher lying excited states created by multi-photon processes during the laser pulse. Similar prompt charge generation was reported in [14]. The subsequent dynamics of PA1 seem to indicate that two different processes take place on different timescales. The very fast initial decay (∼2 ps after photoexcitation), also observed in other conjugated polymers, has been previously assigned to geminate recombination of charges (intra-chain) [14, 15]. Only those charges that are able to escape from this initial geminate pair formation have the chance to recombine non-geminately (inter-chain) leading to the second and slower decay. In addition a slow rise of PA1 is evident on a timescale of ∼100 ps. This feature can be attributed to the diffusion limited dissociation of singlet excitons, for example at defect sites, to generate non-geminate polaron pairs.

We note that the fast decay visible in PA1 is not present in PB. No similar decay can be seen in the PB signal even for shorter timescales. Since PB is an overall signal containing contributions from all of the excited states, this observation implies that the geminate polaron pairs responsible for the initial amplitude of PA1 do not recombine to the ground state (which would induce a fast change in PB), but instead most likely recombine to the singlet exciton. PB is expected to reflect only the dynamics of singlet exciton recombination, modified by the slow recombination of non-geminate polarons to the ground state. The similar dynamics of PB and PA2 are therefore quite compatible with the assignment of PA2 to singlet excited state absorption. In further support of this, a fast rise in PA2 is visible at short times (not easily distinguished on this timescale, but more evident on shorter timescales not shown here), as would be expected for singlet exciton regeneration by the geminate charge pair recombination. We shall see below that both PB and PA2 bands also appear to contain contributions from polaron absorption.

2.2. Red F:PCBM (10 mol% PCBM in Red F)

Figure 5 shows the $\Delta T/T$ spectra of the Red F:PCBM (10 mol% PCBM) blend for the same time delays as in figure 2 plus an additional 400 fs pump–probe delay. The same three main features are also observed for the blend, but their behaviour is completely different. Figure 6 shows the decay of the three features and fits to the decaying tails with exponential functions with different lifetimes. Let us first consider PA1. Although the initial amplitude of PA1 is similar to that in the case of pristine Dow Red F, indicating a similar efficiency of prompt polaron pair generation, the decay of PA1 is now much slower than before. (The tail is fitted by a slow decay of lifetime $\tau = 452$ ps.) The initial fast decay that was assigned to geminate pair recombination in the case of the pristine polymer is now absent. We interpret this as a result of fast electron transfer from negative Red F polarons to PCBM molecules, replacing the short-lived geminate polaron pairs and longer lived non-geminate polaron pairs with longer lived, heterogeneous Red F^+–$PCBM^-$ charge pairs. The presence of PCBM thus enhances charge transfer and stabilizes the charge separated state. Over the next ∼100 ps, bimolecular recombination of these charge pairs competes with slow charge pair generation by diffusion limited dissociation of singlet excitons, resulting in a plateau region. At longer times the slow decay of PA1 is attributed to bimolecular recombination. The rather slower decay than in the pristine polymer suggests that bimolecular recombination is slower for the heterogeneous charge pairs than for the non-geminate Red F polaron pairs.

The PA2 signal now contains both a fast ($\tau_1 = 3.47$ ps) and a slow ($\tau_2 = 365$ ps) component. The fast component can be explained by the disappearance of singlet excitons through dissociation (which may be diffusion limited) and the failure to regenerate these from geminate polaron pair recombination. Independent studies of this system showed that the current generated by photoexciting the polymer is strongly dependent on PCBM

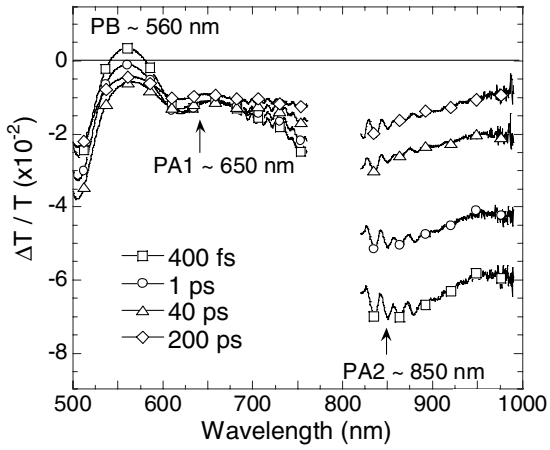

Figure 5. $\Delta T/T$ spectra of Dow Red F:PCBM (10 mol% PCBM in Red F) for different time delays between the pump and probe beams. The data were measured at room temperature. The intensity of the pump beam was $I_{\mathrm{PUMP}} \sim 250\ \mu\mathrm{J\ cm}^{-2}$ at an excitation wavelength $\lambda_{\mathrm{exc}} = 390$ nm. The pump pulse duration was 150 fs.

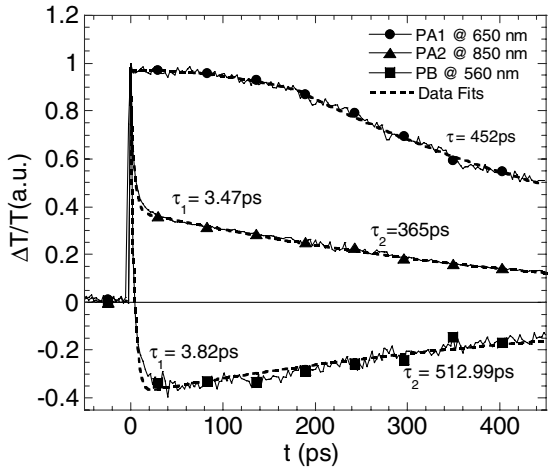

Figure 6. Dynamics of the features observed in the $\Delta T/T$ spectra for a Dow Red F:PCBM (10 mol% PCBM in Red F) blend. The lifetimes obtained by fitting the experimental results to different exponential decays are also shown as are the fits (dashed curves). The dynamics were normalized by using the experimentally measured data at $t = 0$; PA2 = 34.5, PB = 37.7, PA1 = 37.2.

concentration [7]. In the same way, the photoluminescence from the polymer is very efficiently quenched by the addition of PCBM in accordance with previous studies on other polymers [16]. Therefore the residual slow phase in the PA2 signal is unlikely to be due to singlet excitons. Instead we assign this phase to absorption by the long lived Red F polarons. The cation absorption spectrum in figure 3 clearly shows absorption extending beyond 850 nm, and the slow dynamics of this phase mirrors the slow decay of the polarons in PA1.

Finally, the dynamics at 560 nm (PB) for the blend shows a completely different behaviour to that for the pristine polymer. For the pristine polymer, the similar dynamics for PB and PA2 suggested that they were dominated by a common process, namely the decay of singlet

excitons to the ground state. After the addition of PCBM, the PB signal shows an initial fast decay and *changes sign* at very small time delays. This cannot be explained by increased polymer ground state absorption. Additionally, the shape of the spectrum is preserved for the blend but it seems to have shifted downwards in amplitude. This can only be explained by the appearance of another absorption feature in this spectral range on top of which the PB signal is superimposed, and such absorption is most likely explained by the presence of a much higher density of charges. We note in this context that the C_{60}^{-} absorption spectrum, which should resemble that of $PCBM^{-}$, shows peaks at 1076 and 952 nm [17] and is therefore unlikely to be responsible for the extra absorbance at 560 nm. The cation absorption of chemically doped Red F is relatively insensitive to doping at 560 nm, but shows some absorption at higher doping levels (figure 3). Because the ground state of the red chromophore is known to absorb at this wavelength [18], a bleaching of the signal would normally be expected here. The absence of a bleaching in the oxidized Red F spectrum may therefore be due to a competing absorption from the positive polaron. The broad negative shift of the spectrum in figure 5 can thus be attributed to a broad absorption by the charge separated positive polaron competing with the bleaching of the ground state at longer delay times, making the PB signal change sign. We note that the competing absorption at 560 nm must be due only to charge separated positive polarons and not to geminate polaron pairs, since no fast decay of PB was observed in the pristine polymer case. The alternative explanation that the $PCBM^{-}$ species do indeed absorb at 560 nm cannot be ruled out, but there is no prior evidence for any absorption by the PCBM radical anion here.

Irrespective of whether the absorption at 560 nm is due to separated Red F^{+} polarons or $PCBM^{-}$ radicals, we can assign the initial decay of the PB signal to the formation of stabilized charge pairs, upon electron transfer from negative Red F polarons to the PCBM. In this way, we can estimate the charge transfer time, τ_{CT}, for an electron to transfer from the polymer to PCBM, by fitting the lifetime of the initial fast decay of PB. τ_{CT} was estimated in this way to be $\tau_{CT} \sim 4$ ps. The dynamics of the PB signal on longer timescales is very similar to that for PA1, supporting the idea that the 560 nm signal has a large contribution from charged states (as per PA1). According to the above assignments, the slow development of PB is the net result of ground state recovery and reduced polaron absorption, both due to slow recombination of charge pairs, and not related to singlet exciton decay.

The τ_{CT} estimated in this work is considerably longer than that reported before for MDMO-PPV:PCBM systems [16]. However, charge transfer is expected to be mediated by an exciton diffusion process and therefore to show a strong dependence on acceptor concentration [19]. In this way, larger concentrations of PCBM lead to much faster charge transfer and correspondingly, for similar concentrations of PCBM, there are similar τ_{CT} [19], even when the electron donor material is changed from MDMO-PPV to Dow Red F. We note also that the slow rise evident in PA1 for the pristine case and the plateau evident in the case of the blend show that charges continue to be generated on very much longer timescales, of the order of 100 ps. Such dynamics can be expected for diffusion limited exciton dissociation, allowing that singlet excitons may be trapped.

3. Model

In order to support the above assignments we have developed a simple rate equation model to simulate the gross features of the dynamics in figures 4 and 6. The basic assumptions of the model are as follows: PA1 is due to positive polaron absorption at 650 nm; PA2 is due to singlet exciton absorption plus a contribution from the positive polarons, but with a lower extinction coefficient than at 650 nm; PB is due to the bleaching of the ground state minus a contribution

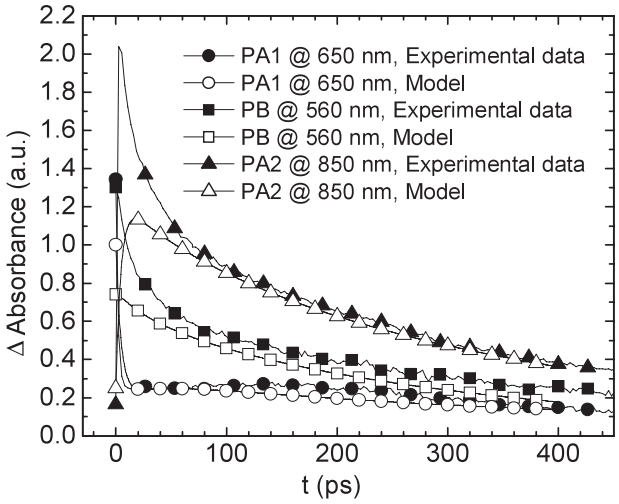

Figure 7. Measured (full symbols) and modelled (open symbols) dynamics of the transient absorption signals PB, PA1 and PA2 (as defined previously) observed in the pristine Dow Red F polymer film. See the text for details of the model and the fitting parameters.

from charge separated positive polaron absorption at 560 nm. Upon initial excitation by the laser, which is assumed intense enough for prompt polaron pair generation, a fraction f_{gem} of excitations result in polaron pair formation and a further fraction f_{sep} result in non-geminate polaron pairs. Subsequently, the following processes occur in the absence of PCBM. Singlet excitons decay to the ground state with a rate constant k_{rad}. (Stimulated emission is not included as previous studies show that stimulated emission only occurs at wavelengths longer than 600 nm in Red F [18].) Geminate polaron pairs recombine to regenerate the singlet exciton with a rate constant k_{gem}. Singlet excitons continue to dissociate in a diffusion limited manner (modelled here as an anomalous diffusion process that would give rise to stretched exponential kinetics in the absence of other processes), giving rise to non-geminate polaron pairs at a rate $A_{\mathrm{pn}}t^{\alpha-1}$. Non-geminate polaron pairs recombine through bimolecular recombination with a coefficient B_{pn} to the ground state. In the presence of PCBM, negative polarons are allowed to undergo rapid electron transfer to create PCBM anions, with a rate constant k_{CT}. Exciton dissociation generates Red F^+–$PCBM^-$ pairs rather than Red F polaron pairs, and the heterogeneous charge pairs recombine bimolecularly to the ground state with a coefficient B_{pC}, which is in general lower than B_{pn}. All other details are identical to the case of the pristine polymer. The rate equations and parameters used are listed in the appendix.

Typical results for the dynamics in the pristine polymer and in the blend are shown in figures 7 and 8. Values for f_{gem} and f_{sep} were estimated from the relative size of the prompt (total polaron) and longer time (non-geminate) PA1 signal in figure 4. k_{rad} and k_{gem} were estimated from the slow decay of PB and the initial fast decay of PA1 in figure 4. k_{CT} was estimated from the fast component of PB, attributed to charge transfer, in figure 6. A_{pn}, A_{pC}, B_{pn} and B_{pC} and the dispersion parameter were estimated from the amplitude and decays of the PA1 phase in each case. The precise values of the parameters are not critical to the general behaviour. Values of relative extinction coefficients were estimated partly from the cation absorption spectrum and partly by trying to fit the dynamics. The values of all parameters used are given in the appendix.

It can be seen that the rate equation model reproduces the main features of the experimental data, indicating that the assignments given above are plausible. Although it is not practical to

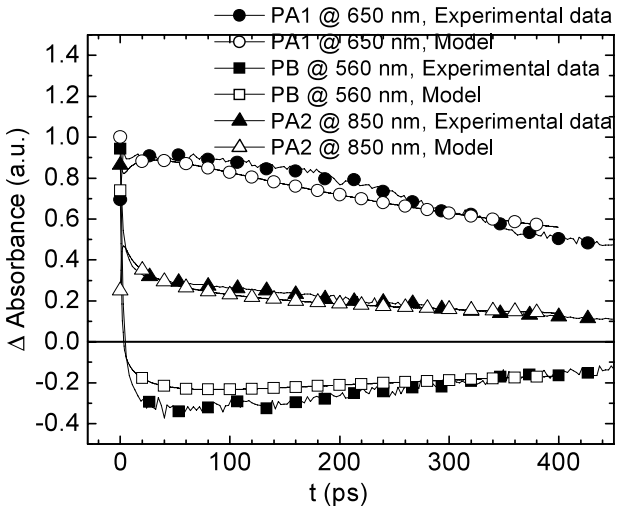

Figure 8. Measured (full symbols) and modelled (open symbols) dynamics of the transient absorption signals PB, PA1 and PA2 (as defined previously) observed in the Dow Red F:PCBM (10% mol PCBM in Red F) blend film. See the text for details of the model and the fitting parameters.

determine the values of all parameters precisely from these data sets, and other combinations of parameters are likely to work equally well, we can make a few important points from our experience using the model. In particular, we find that:

(i) It is essential to include both prompt ($<$1 ps) and slower ($\sim$100 ps) polaron generation to explain the dynamics in both cases.
(ii) The main difference between the dynamics for the pristine polymer and for the blend is in the efficiency with which prompt polarons are converted into long lived charges. The timescale for this charge transfer conversion is a few picoseconds.
(iii) A contribution from polaron absorption is required to explain the dynamics of all three bands, particularly in the case of the blend.
(iv) The recombination of polaron pairs is slower in the blend than in the pristine polymer.
(v) Geminate polarons appear to recombine to the singlet exciton, but longer lived charges must recombine to the ground state.

It is clear that the model does not reproduce a fast phase visible in the dynamics of PB and PA2 in the case of the pristine polymer. This may be due to an additional exciton decay process, apart from k_{rad}, possibly enabled through the high initial exciton densities. We do not attempt to introduce an additional process to model this, judging that it is not critical to the charge transfer kinetics studied here.

4. Summary

In summary, we have used ultrafast spectroscopy to identify early-stage species created upon photoexcitation of Dow Red F:PCBM blends and have studied their decay dynamics. Charge transfer takes place fairly soon after photoexcitation ($\sim$4 ps) and the process lasts for around 120 ps (the growth time of the polaron signal). The resulting absorption features have been assigned to charged polaron states. The excitons created by photoexcitation thus dissociate

with the positive charges left on polymer chains and the negative charges transferred to the fullerene. These separated charges have the potential to produce a very useful photocurrent that can be used for device applications in photodetection and solar energy conversion.

Acknowledgments

We thank The Dow Chemical Company for providing the Dow Red F polymer used in these experiments and The UK Engineering and Physical Sciences Research Council (GR/M45115) for financial support. RP and DDCB acknowledge further support from the European Community—Access to Research Infrastructure action of the Improving Human Potential Programme, contract No HPRI-CT-2001-00148 (Centre For Ultrafast Science and Biomedical Optics, CUSBO). RP also thanks the Imperial College London Centre for Electronic Materials and Devices (CEMD) for a student bursary.

Appendix. The rate equation model

A.1. The rate equation model for pristine polymer

For the pristine polymer the rate equations (A.1)–(A.4) were solved for the density of singlet excitons (S_1), the bleaching of the ground state (ΔS_0), the density of geminate polaron pairs ($P_{\rm gem}$), charge separated positive polarons $P_{\rm p}$ and charge separated negative polarons ($P_{\rm n}$). The initial conditions were that $\Delta S_0 = -1$, $S_1 = 1 - f_{\rm gem} - f_{\rm sep}$, $P_{\rm gem} = f_{\rm gem}$ and $P_{\rm p} = P_{\rm n} = f_{\rm sep}$ at $t = 0$.

Singlet excitons decay by radiation and dissociation after diffusion, and are replenished by geminate pair recombination:

$$\frac{{\rm d}S_1}{{\rm d}t} = -k_{\rm rad}S_1 - A_{\rm pn}t^{\alpha-1}S_1 + k_{\rm gem}P_{\rm gem}. \tag{A.1}$$

The bleaching of the ground state is restored by singlet exciton decay and the recombination of separated charge pairs:

$$\frac{{\rm d}\Delta S_0}{{\rm d}t} = k_{\rm rad}S_1 + B_{\rm pn}P_{\rm p}P_{\rm n}. \tag{A.2}$$

Intra-chain (geminate) polaron pairs recombine:

$$\frac{{\rm d}P_{\rm gem}}{{\rm d}t} = -k_{\rm gem}P_{\rm gem}. \tag{A.3}$$

Non-geminate pairs of Red F^+ polarons and Red F^- polarons are generated by dissociation of singlet excitons after diffusion, and recombine with each other in a bimolecular manner:

$$\frac{{\rm d}P_{\rm p}}{{\rm d}t} = \frac{{\rm d}P_{\rm n}}{{\rm d}t} = A_{\rm pn}t^{\alpha-1}S_1 - B_{\rm pn}P_{\rm p}P_{\rm n}. \tag{A.4}$$

The constants $k_{\rm rad}$, $k_{\rm gem}$, $B_{\rm pn}$ and $f_{\rm pn}$ are defined in the text. $A_{\rm pn}$ is a constant proportional to the anomalous diffusion rate and the exciton dissociation probability and α is the dispersion parameter for the anomalous diffusion of singlet excitons. In the absence of any competing process this would lead to stretched exponential singlet exciton decay kinetics of the form $S_1 \sim \exp(-(t/\tau)^{\alpha})$. We note that it is not necessary to assume anomalous diffusion to obtain the general dynamics obtained here, but the model gives a better fit to the shape of the dynamic curves, and is expected for energy diffusion in disordered systems.

The transient optical densities of the three bands are determined from the excited state populations as follows:

$$\Delta \mathrm{OD}_{\mathrm{PB}} = -\epsilon_{\Delta S_0} \Delta S_0 - \epsilon_{P560} P_{\mathrm{p}} \tag{A.5}$$

$$\Delta \mathrm{OD}_{\mathrm{PA1}} = \epsilon_{P650}(P_{\mathrm{gem}} + P_{\mathrm{p}}) \tag{A.6}$$

$$\Delta \mathrm{OD}_{\mathrm{PA2}} = \epsilon_{S_1} S_1 + \epsilon_{P850} P_{\mathrm{p}} \tag{A.7}$$

where $\epsilon_{\Delta S_0}$, ϵ_{S_1}, ϵ_{P560}, ϵ_{P650} and ϵ_{P850} represent the relative extinction coefficients of the ground state at 560 nm, the singlet exciton at 850 nm and the positive polaron at 560, 650 and 850 nm respectively.

A.2. The rate equation model for the blend

For the blend, exactly the same model is used with the following changes:

(i) Negative polarons on Red F (geminate and non-geminate pairs) transfer to PCBM molecules with the rate constant k_{CT}.
(ii) Dissociation of singlet excitons following diffusion leads to charge separated pairs of Red F^+ and $PCBM^-$ (rather than Red F^+ and Red F^-) and the probability of generating such a charge pair is increased by the factor $A_{\mathrm{pC}}/A_{\mathrm{pn}}$.
(iii) Red F^+–$PCBM^-$ polaron pairs recombine by bimolecular recombination with a rate coefficient B_{pC} (in general) slower than the B_{pn} for Red F polaron pair recombination.

The rate equations then become

$$\frac{\mathrm{d}S_1}{\mathrm{d}t} = -k_{\mathrm{rad}} S_1 - A_{\mathrm{pC}} t^{\alpha-1} S_1 + k_{\mathrm{gem}} P_{\mathrm{gem}} \tag{A.8}$$

$$\frac{\mathrm{d}\Delta S_0}{\mathrm{d}t} = k_{\mathrm{rad}} S_1 + B_{\mathrm{pC}} P_{\mathrm{p}} C_{\mathrm{n}} \tag{A.9}$$

$$\frac{\mathrm{d}P_{\mathrm{gem}}}{\mathrm{d}t} = -k_{\mathrm{gem}} P_{\mathrm{gem}} - k_{\mathrm{CT}} P_{\mathrm{gem}} \tag{A.10}$$

$$\frac{\mathrm{d}P_{\mathrm{p}}}{\mathrm{d}t} = k_{\mathrm{CT}} P_{\mathrm{gem}} + A_{\mathrm{pC}} t^{\alpha-1} S_1 - B_{\mathrm{pC}} P_{\mathrm{p}} C_{\mathrm{n}} \tag{A.11}$$

$$\frac{\mathrm{d}P_{\mathrm{n}}}{\mathrm{d}t} = -k_{\mathrm{CT}} P_{\mathrm{n}} \tag{A.12}$$

with an additional rate equation to describe the evolution of negative PCBM polarons, C_{n}:

$$\frac{\mathrm{d}C_{\mathrm{n}}}{\mathrm{d}t} = k_{\mathrm{CT}} P_{\mathrm{gem}} + k_{\mathrm{CT}} P_{\mathrm{n}} + A_{\mathrm{pC}} t^{\alpha-1} S_1 - B_{\mathrm{pC}} P_{\mathrm{p}} C_{\mathrm{n}} \tag{A.13}$$

where the initial condition is $C_{\mathrm{n}} = 0$ at $t = 0$.

The values of the parameters used in figures 7 and 8 are as follows. Rate constants: $k_{\mathrm{rad}} = 0.002\ \mathrm{ps}^{-1}$, $k_{\mathrm{gem}} = 0.2\ \mathrm{ps}^{-1}$, $k_{\mathrm{CT}} = 0.5\ \mathrm{ps}^{-1}$, $B_{\mathrm{pn}} = 0.02\ \mathrm{conc.\ unit}^{-1}\ \mathrm{ps}^{-1}$ and $B_{\mathrm{pC}} = 0.002\ \mathrm{conc.\ unit}^{-1}\ \mathrm{ps}^{-1}$. Initial concentrations: $f_{\mathrm{gem}} = 0.8$, $f_{\mathrm{sep}} = 0.2$. Diffusion parameters: $\alpha = 0.5$ and charge generation coefficients $A_{\mathrm{pn}} = 0.14\ \mathrm{ps}^{-1/2}$ and $A_{\mathrm{pC}} = 0.7\ \mathrm{ps}^{-1/2}$. Relative extinction coefficients: $\epsilon_{\Delta S_0} = 1$, $\epsilon_{S_1} = 1.5$, $\epsilon_{P560} = 1.3$, $\epsilon_{P650} = 1$ and $\epsilon_{P850} = 0.25$. We stress here that the goal of this modelling was to demonstrate that the observed dynamics are consistent with the physical model proposed, and not to determine the parameters controlling the processes to any high precision. The parameters have not been optimized, and we accept that other parameter combinations may fit the data equally well.

References

[1] Schilinsky P, Waldauf C and Brabec C J 2002 *Appl. Phys. Lett.* **81** 3885
[2] Winder C, Matt G, Hummelen J C, Janssen R A J, Sariciftci N S and Brabec C J *Thin Solid Films* **403** 373
[3] Padinger F, Rittbergr R S and Sariciftci N S 2003 *Adv. Funct. Mater.* **13** 85
[4] Redecker M, Bradley D D C, Inbasekaran M, Wu W W and Woo E P 1999 *Adv. Mater.* **11** 241
[5] Campbell A J, Bradley D D C and Antoniadis H 2001 *Appl. Phys. Lett.* **79** 2133
[6] Pacios R, Nelson J, Bradley D D C and Brabec C J 2003 *Appl. Phys. Lett.* **83** 4764
[7] Pacios R, Nelson J, Bradley D D C and Brabec C J 2003 *Synth. Met.* **137** 1469
[8] Inganas O, Svensson M, Zhang F, Gadisa A, Persson N K, Wang X and Andersson M R 2004 *Appl. Phys.* A **79** 31
[9] Vardeny Z V and Wei X 1997 *Handbook of Conducting Polymers* (New York: Dekker)
[10] Stevens M A, Silva C, Russell D M and Friend R H 2001 *Phys. Rev.* B **63** 5213
[11] Virgili T, Cerullo G, Lüer L, Lanzani G, Gadermaier C and Bradley D D C 2003 *Phys. Rev. Lett.* **90** 247402
[12] Kraable B, Klimov V I, Kohlman R, Xu S, Wang H and McBranch D W 2000 *Phys. Rev.* B **61** 8501
[13] Xu S, Klimov V I, Kraable B, Wang H and McBranch D W 2001 *Phys. Rev.* B **64** 193201
[14] Lüer L, Egelhaaf H J, Oelkrug D, Gadermaier C, Cerullo G and Lanzani G 2003 *Phys. Rev.* B **68** 155313
[15] Lüer L, Cerullo G, Zavaleni-Rossi M and Lanzani G 2003 *Chem. Phys. Lett.* **381** 751
[16] Brabec C J, Zerza G, Cerullo G, De Silvestri S, Luzzati S, Hummelen J C and Sariciftci N S 2001 *Chem. Phys. Lett.* **340** 232
[17] Kato T, Kodama T, Shida T, Nakagawa T, Matsui Y, Suzuki S, Shiromaru H, Yamauchi K and Achiba Y 1991 *Chem. Phys. Lett.* **180** 446
[18] Ruidong X, Heliotis G and Bradley D D C 2003 *Appl. Phys. Lett.* **82** 3599
[19] Haugeneder A, Neges M, Kallinger C, Spirkl W, Lemmer U, Feldmann J, Scherf U, Harth E, Gügel A and Müllen K 1999 *Phys. Rev.* B **59** 15346